W. Dolan[1], T. M. Pavelsky[1], and X. Yang[1]

[1]University of North Carolina at Chapel Hill

Corresponding author: Wayana Dolan (whyana@live.unc.edu)

Key Points:

- Remotely-sensed water color is indicative of functional lake connectivity in high-sediment Arctic deltas
- Functional connectivity is related to temporal variations in discharge and spatial variations in lake surface elevation
- Differences in functional connectivity drive lake ice phenology, which is likely important for photochemical processes
-

Abstract

Within Arctic deltas, surficial hydrologic connectivity of lakes to nearby river channels influences physical processes like sediment transport and ice phenology as well as biogeochemical processes such as photochemistry. As the Arctic hydrologic cycle is impacted by climate change, it is important to quantify temporal variability in connectivity. However, current connectivity detection methods are either spatially limited due to data availability constraints or have been applied at only a single time step. Additionally, the relationship between connectivity and lake ice is still poorly quantified. In this study, we present a multitemporal classification and validation of lake connectivity in the Colville River Delta, AK. We introduce a connectivity detection algorithm based on remote sensing of water color that is expandable to other high-sediment Arctic deltas. Comparison to validation datasets suggests that detection of high vs. low connectivity lakes is accurate in 69.5–85.5% of cases. Connectivity temporally varies in about 20% of studied lakes and correlates strongly with discharge and lake elevation, supporting the idea that future changes in discharge will be drivers of future changes in connectivity. Lakes that are always highly connected start and end ice break up an average of 26 and 16 days earlier, respectively, compared to lakes that are never connected. Because spring and summer ice conditions drive Arctic lake photochemistry processes, our research suggests that surface connectivity is an important parameter to consider when studying biogeochemistry of Arctic delta lakes.

Plain language summary

Arctic deltas contain a complex tapestry of channels and lakes. Lakes can be isoloated from channels or connected to channels—either by feeder channels, other lakes, or by water movement over land during flooding. This connectivity is important because it impacts the movement of sediment and animals, light penetration through water, and when lake ice forms and disappears. While we anticipate future changes in connectivity due to climate change, our ability

to monitor connectivity is limited to individual deltas or single instances in time. Additionally, the relationship between lake ice and connectivity is poorly understood. In this study, we used a method based on satellite observations of water color to examine lake connectivity variations within the Colville River Delta, AK. We found that most lakes stay connected or disconnected, but that about 20% of lakes have variable connectivity. These lakes are more likely to be connected when river discharge is high. Additionally, lake ice tends to break up earlier and last for a shorter period of time in connected lakes. Because lake ice conditions drive chemical interaction between sunlight and organic compounds in the water, connectivity is important to consider when studying the biology and chemistry of Arctic delta lakes.

1. Introduction

Arctic deltaic floodplains consist of complex river and lake systems that transport and store both inorganic and organic materials. The connectivity of Arctic floodplain lakes to nearby channels determines how much river water these lakes receive each year (Marsh & Hey, 1989; Lesack et al., 1998; Lesack & Marsh, 2010; Piliouras & Rowland, 2020). This interaction, in turn, influences carbon storage and ecological productivity and diversity (Wiklund et al., 2012; Lesack & Marsh, 2010). As the Arctic hydrological cycle intensifies due to climate change (Dai et al., 2009; Bring et al., 2017), it is important to quantify the impact of these changes on connectivity so that we can better understand patterns of carbon transport, carbon emission, and biological diversity in these deltaic ecosystems. These relationships are particularly vital because deltas are the interface between changing river systems and changing oceans, mediating the amount of terrestrial sediment and carbon exported into the coastal ocean (Emmerton et al., 2008; Piliouras & Rowland, 2020).

While there are many types of hydrologic connectivity (e.g. Covino, 2017), delta lakes are functionally connected to river channels when they are recharged with high sediment river water, which changes their physical, ecological, and biogeochemical properties. Within deltas, variations in functional lake connectivity lead to noticeable changes in lake biogeochemistry. High functional connectivity lakes, by definition, receive more river water each year, leading to shorter water residence times (Coops et al., 1999; Coops et al., 2008) and increased suspended sediment concentrations (SSC, Lesack & Marsh, 2010; Long & Pavelsky, 2013). The higher level of SSC leads to decreased light penetration, predominantly inorganic lake sediments, and low macrophyte productivity (Lesack et al., 1998; Lesack & Marsh, 2010). Arctic lakes are a significant contributor of greenhouse gases to the atmosphere (e.g. Phelps et al., 1998; Walter Anthony et al., 2010; Boereboom et al., 2012; Karlsson et al., 2013), so these connectivity-driven differences are also important from a carbon cycle perspective. Poorly or sporadically connected lakes have higher organic material and macrophyte productivity, resulting in increased dissolved organic carbon (DOC) compared to their high functional connectivity counterparts (Amoros & Bornette, 2002; Tank et al., 2009; Lesack & Marsh, 2010). However, this same macrophyte productiv-

ity can reduce CO_2 emission to the atmosphere due to increased photosynthesis (Tank et al., 2009).

Functional connectivity also impacts the properties of lake ice. While research on the relationship between lake ice and connectivity is in its early stages, several observations suggest that connectivity may be a driving factor in intraregional lake ice timing. First, as observed in Canada's Mackenzie River Delta during the Fall freeze-up period, connected lakes are more likely to be impacted by water movement from lakes to channels. This water movement results in lower water levels, increased likelihood of bottom-fast ice, and decreased lake bottom temperatures during the winter (Ensom et al., 2012). Additionally, Howell et al. (2009) demonstrate that riverine input to Great Slave Lake in Canada acts as a thermal and mechanical trigger for earlier lake ice breakup near the river input site. In a study of Alaskan lakes, Arp et al. (2013) found that while air temperature and lake area explained 80% of the variance in ice-out timing, they hypothesize that connectivity may be a driving force behind additional variability in ice-out timing within regions, but emphasize the need for further studies focusing directly on investigating the topic.

Lake ice is particularly important from a biogeochemical standpoint because it is an effective blocker of light (Vione & Scozzaro, 2019). Earlier ice-out timing is very effective at increasing light availability to the lacustrine water column because it usually occurs during the late spring/early summer maximum in solar radiation (Vione & Scozzaro, 2019). A relationship between ice timing and connectivity would thus drive differences in aquatic photochemistry based on lake connectivity. The relationship between connectivity and lake ice is also potentially important from a methane standpoint. Within ice-covered lakes, greenhouse gasses, particularly methane, accumulate under and within ice and are released to the atmosphere as a large pulse during breakup (Phelps et al., 1998; Karlsson et al., 2013; Denfeld et al., 2018). Connectivity-impacted changes in ice timing could influence the timing of this pulse. Also, analysis of four lakes in Sweden (Boereboom et al., 2012) found that a lake connected via channel to the river network had almost no methane bubbles trapped in the ice. This contrasted with the other three lakes that were rich in methane bubbles and that were either completely isolated or only connected via channel to another lake. Thus, understanding a delta lake's functional connectivity is essential to understanding its physical characteristics, and, by extension, its biogeochemistry.

Despite the importance of connectivity in deltaic ecosystems, previous studies have focused largely on either relatively small scales, a single time step, or both. Prior research has used *in situ* data (e.g. Remmer et al., 2020), remote sensing (e.g. Pilliouras & Rowland, 2020), or a combination of the two (e.g. Marsh & Hey, 1989; Lesack & Marsh, 2010; Long & Pavelsky, 2013) to identify lake connectivity. One common method of connectivity identification involves pairing discharge records with lake sill elevations calculated via aerial imagery (e.g. Marsh & Hey, 1989; Lesack & Marsh, 2010). While this method effectively

combines current lake sill elevations and historical discharge records to study past connectivity, it assumes that sill elevations are stable over time, which may not hold true given increased erosion and deposition due to permafrost loss in Arctic deltas (e.g. Lauzon et al., 2019). Additionally, because this method requires high resolution aerial surveys or fieldwork to determine lake sill elevations, it is challenging to apply on large scales across multiple deltas. In contrast, Pilioura & Rowland (2020) used Landsat (30m resolution) imagery to detect the presence of channel connections between lakes and the main channel network. While this works very well for lakes connected with large channels, and is scalable across deltas and time periods, it is unable to detect connectivity driven by channels narrower than 30m or connectivity driven by flood-induced overland flow.

In this paper, we seek to understand the variability of lake-to-channel connectivity over decadal scales, including both channel and overland flow connectivity. We develop and test our algorithm within the Colville Delta, AK because there is ample validation data available there. Our work is organized into four research questions and corresponding experiments:

> *Q1: How well can Landsat-derived observations of water color detect functional connectivity in the Colville Delta, even when channels are sub-pixel in width?*

In this experiment, we compare Landsat-derived lake connectivity classifications (high functional connectivity vs low functional connectivity) to three validation datasets and assess classification accuracy.

> *Q2: How many lakes in the Colville Delta have static connectivity versus variable connectivity over the twenty-year study period?*

In this experiment, we classify functional lake connectivity within 5-year periods (2000-2004, 2005-2009, 2010-2014, 2015-2019).

> *Q3: How much of an impact do elevation and discharge have on functional lake connectivity in the Colville Delta?*

In this experiment, we classify and then compare functional lake connectivity within five high maximum discharge years and five low maximum discharge years. Additionally, we compare lake connectivity during a five-year time period to lake surface elevations.

> *Q4: What are the impacts of connectivity on lake ice?*

In this experiment, we compare 20-year lake ice climatology records to our connectivity classifications and discuss the implications of ice cover and connectivity on biogeochemistry.

2. Study area

The Colville River originates in the Brooks Range, flows west to east across the North Slope, and then about 20 km downstream of Umiat, AK, takes a

northward turn and proceeds ~140 km into the Beaufort Sea. The entire Colville River Basin is underlain by continuous permafrost (Walker, 1998; Mikhailova, 2009), except for a few taliks under deep lakes and deeper parts of distributary channels within the delta (Walker et al., 1987). The delta itself is lake-rich and estimates of its size range from 550–665 km^2 (Mikhailova, 2009). While recent estimates of sediment concentrations are limited, observations from the late 1990s indicate that the Colville River Delta has one of the highest annual suspended sediment loads compared to other large Arctic rivers, with a 1998 estimate of 97 $tkm^{-2}y^{-1}$, compared, for example, to the Yukon (70 $tkm^{-2}y^{-1}$) and the Mackenzie (24 $tkm^{-2}y^{-1}$) river deltas (Walker, 1998). The delta channels and delta lakes remain frozen from approximately late September/early October to late May/mid-June, when the spring discharge maximum drives river ice breakup (Mikhailova, 2009). While the delta itself only receives 300–400mm of precipitation each year (Mikhailova, 2009), historical records show that river water level can increase by 3–5m during breakup, inundating at least 65% of the delta's total area (Walker, 1975).

We acknowledge that, first and foremost, the Colville River Delta is home to the village of Nuiqsut, an Iñupiat, or, more specifically, a Kuukpikmiut (people of the Colville River) community (population 492 as of 2020; Department of Commerce, Community, and Economic Development, 2021). Subsistence activities are one of the primary industries of the village, including fishing, hunting, and whaling (Brubaker et al., 2014). Both traditional knowledge and quantitative climate data paint a picture of a changing delta, with temperatures rapidly increasing (Brubaker et al., 2014; Applied Climate Information System). For example, during the study period for this analysis (2000–2019), mean annual air temperature in Nuiqsut increased by an average 0.15℃ per year (same results using both a linear model and Sen's slope, $p<0.05$ for both), with larger temperature changes in the late winter months such as February (Sen's Slope: 0.42℃/yr, Linear Slope: 0.37℃/yr) (Applied Climate Information System). Residents share that thaw of permafrost below lakes has led to lake draining and drying (Brubaker et al., 2014). This change in permafrost, in combination with later ice freeze-up, earlier ice breakup, and prolonged active layer thaw have reportedly led to dangerous travel conditions both on land (mushy conditions that are bad for snowmobiles) and over water (shorter and less stable ice season) (Brubaker et al., 2014). Residents also express concern with loss of habitat due to lake draining as well as loss of accessibility to certain fishing locations due to channels drying up and reducing connectivity (Brubaker et al., 2014). However, more frequent extreme events, such as elevated flood water levels (Brubaker et al., 2014), could potentially result in increased short-duration connectivity.

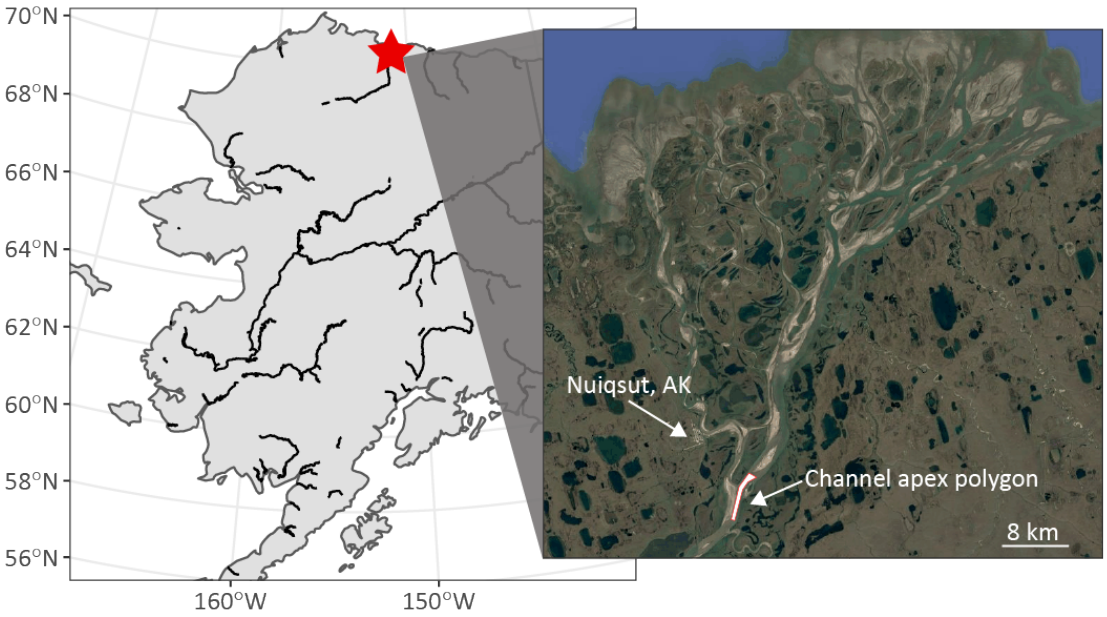

Figure 1. Location of the Colville River Delta on the North Slope of Alaska. Black lines are river reaches wider than 150m contained in the GRWL summary database (Allen & Pavelsky, 2018). Delta shown in inset, highlighting the channel apex polygon, and the village of Nuiqsut, AK.

3. Methods

3.1. Datasets

3.1.1. Development of Landsat Water Masks

To create water masks based on Landsat imagery, we use summertime (June–September) Landsat 5/7/8 Tier 1 Surface Reflectance imagery from 2000–2019. Landsat 7 imagery is only used prior to scan line corrector failure (5/31/2003). To reduce noise from clouds and snow/ice, we use only those Landsat scenes that are less than 75% cloudy overall. We further remove pixel-level cloud and cloud shadow influence using bits 3 (cloud shadow) and 5 (cloud) of the quality band ('pixel_qa'), and we use bit 4 to remove snow/ice. Additionally, we use the DSWE algorithm to select only high confidence water pixels in each image (Jones, 2019). Lastly, we remove pixels with unreasonable reflectance values (values $> 10{,}000$ or values < 0). We refer to images that have gone through this process as 'filtered Landsat images.'

3.1.2. Lake boundaries

To select initial lakes for analysis, we use lakes from the Alaskan Lakes Database (Wang et al., 2011) that contain at least 100 pixels classified as water 90% of the time and are within the bounds of the Colville Delta (Pekel et al., 2016, n=120 lakes). Note that we have split up several large lake complexes that were

originally grouped into one polygon into single lake polygons. After splitting, these lakes are referred to as the 'study lakes.'

3.1.3. Validation datasets

We compare lake connectivity classification results against three different lake connectivity datasets to assess accuracy. First, we use the high resolution (<10m) Google Earth Composite Image (GECI) (a composite of 2013–2016 imagery) to manually identify those lakes that have a visible channel connection. Lakes whose channel connection is unclear (e.g. lakes that look like they have a dry channel that perhaps could fill up during floods) are marked as 'uncertain channel connection.'

Second, we compare connectivity classifications against a 1992 survey of the Colville Delta (Jorgenson et al., 1997). This dataset was contained in an image in the manuscript and we digitized each lake's classification by hand. Lakes in this dataset that correspond with our study lakes are classified into the following categories (full descriptions can be found in Table 4 of Jorgenson et al., 1997):

Medium-High connectivity

- *Deep connected lake:* Lakes 1.5m in depth that commonly have long, narrow, and persistent connections to the delta channel network.
- *Deep tapped lake w/ high-water connection:* Lakes 1.5m in depth that have been 'tapped' by erosion of adjacent river banks. Connecting channels are dry unless discharge is high.
- *Deep tapped lake w/ low-water connection:* Same as prior, but connection channels are filled with water, even at low discharge.
- *Shallow tapped lake w/ high-water connection:* Lakes < 1.5m in depth that have been 'tapped' by erosion of adjacent river banks. Connecting channels are dry unless discharge is high.
- *Shallow tapped lake w/ low-water connection:* Same as prior, but connection channels are filled with water even at low discharge.

No connectivity

- *Deep isolated lake:* Lakes 1.5m in depth that have no distinct outlets and are not connected to the channel network.
- *Shallow isolated pond:* Lakes <1.5m in depth with no distinct outlets or channel connections.

No connectivity data available

- *Brackish ponds:* Shallow ponds near the delta toe that may be impacted by very high tides or storm surges. May or may not have connections to the channel network.

Lastly, we compare connectivity classifications to the channel presence/absence classification by Piliouras & Rowland (2020) based on summer Landsat images in 2014. This dataset is stored in an image in which waterbodies that are connected to the channel network have values of 1 and waterbodies that are not connected are masked out of the image. Data was initially contained in a MATLAB Data File and was converted to TIF using R. We then uploaded the TIF to Google Earth Engine. In Google Earth Engine, we negatively buffered the study lake polygons by one Landsat pixel (30m), and then counted how many connected water body pixels were inside each buffered lake polygon. If more than or equal to 10 connected waterbody pixels fell within the lake polygon, the lake was considered connected in the validation data set. If there were fewer than 10 connected pixels, the lake was considered not connected. A threshold of 10 was used to further account for any differences in lake shorelines between our study lake polygons and the validation dataset

3.1.4. ArcticDEM

We investigate patterns between connectivity and lake surface elevation using 2m-resolution ArcticDEM strip data (Porter et al., 2018). ArcticDEM data is only available when there is sunlight, eliminating data availability in winter months. In contrast, the ArcticDEM processing method is not effective over open water. As a result, there is a small window of time each year in which lake elevation data from ArcticDEM is regularly available in this region—the month of April. Therefore, the lake surface elevation in this study represents the elevation of the top of the snow/ice on the lake as opposed to the water surface. There are two years of ArcticDEM data that have complete April observations of the delta: 2015 and 2017. For each of these years, we create an April mean elevation image composite from the ArcticDEM strips. Next, to remove non-water pixels from lake surfaces, we negatively buffer each lake polygon by two Landsat pixels (60m). This removes a lake from analysis that is less than two Landsat pixels wide and reduce the potential contamination of land elevation from mixed water-land pixels.

3.1.5. River discharge data

To analyze the impact of discharge on connectivity, we use daily discharge data from the USGS Gage No. 15875000 at Umiat, AK to identify the top five maximum summer discharge years and the bottom five maximum summer discharge years between 2003, when the station began collecting data, and summer 2019. Maximum summer discharge each year is defined as the highest daily summer (June–September) discharge. While this station is ~125 km upstream from the delta, the Colville River has already drained approximately 67% of its catchment area (U.S. Geological Survey; Walker & Hadden, 1998) by the time the river waters reach the station. We assume that these extreme discharge years are likely the same at Umiat, AK and within the delta itself.

3.2. Detection of connectivity

In this study, we differentiate functionally connected and functionally discon-

nected lakes based on their colors relative to the color of the river entering the delta. We start by extracting Landsat reflectance measurements for lakes and river channels (Section 3.2.1.), then calculate the water color for each observation (Section 3.2.2.). Finally, using density distribution of the ratio between lake and channel color (Section 3.2.3.), we calculate clusters of observations that correspond to connected and disconnected lakes (Section 3.2.4.).

3.2.1. Extraction of paired lake and channel water color observations

The first step in this analysis is to match up same day filtered Landsat observations of each lake to filtered Landsat observations of the channel at the apex of the delta (**Figure 1, inset**). For each filtered Landsat observation of each study lake, we calculate the mean value of each visible RGB band. We do the same thing for the river channel polygon at the apex of the delta (**Figure 1**). To ensure that there are enough pixels to accurately complete our analysis, we then remove daily observations if the mean RGB values were calculated using fewer than 100 cloud-free water pixels. Lastly, we temporally match up same-day channel and lake observations, and we remove observations that do not have a same-day match. If there is more than one-same day match, which commonly occurs at the edge of Landsat tiles, we only keep the match with the smallest difference in time between lake and channel observations.

3.2.2. Calculation of water color

To differentiate functionally connected and disconnected lakes, we take advantage of the difference in color between high sediment river water and lower sediment lake water to identify high sediment river water recharge of deltaic lakes. We use the algorithm by Wang et al. (2015) to convert remotely sensed RGB values to dominant wavelength (λ_d) values within the visible range of 380 to 700 nm. This method was developed to study lake water color using MODIS imagery and has also been used to study river color using Landsat imagery (Gardner et al., 2021) and lake color using Sentinel-2 imagery (Giardino et al., 2019).

To calculate λ_d, we first calculate tristimulus values using the RGB reflectance values:

$$X = 2.7689R + 1.7517G + 1.1302B$$

$$Y = 1.0000R + 4.5907G + 0.0601B$$

$$Z = 0.0565G + 5.5943B$$

Next, we convert these tristimulus values to chromaticity coordinates (x,y,z).

$$x = \frac{X}{X+Y+Z}$$

$$y = \frac{Y}{X+Y+Z}$$

$$z = \frac{Z}{X+Y+Z}$$

However, to display the color data in two dimensions, x and y are often plotted on chromaticity diagrams (e.g. Wang et al., 2015: Figure 4), and a separate value, the hue angle(α), is calculated using the following equation to identify λ_d on the chromaticity diagram:

$$\alpha = (arctan2 \cdot \frac{x - 0.3333}{y - 0.3333}) \frac{180}{\pi}$$

For our purposes, using the hue angle (α) and the chromaticity coordinates (x,y), we use a reference lookup table developed by Wang et al. (2015) to find the dominant wavelength (λ_d) that represents the wavelength that the human eye would see given the RGB values observed by the satellite.

3.2.3. Calculation of dominant wavelength ratios

For each paired observation of lake and channel, we calculate the ratio between λ_d of the lake and λ_d of the channel, which we refer to as the dominant wavelength ratio. If the ratio is larger than 1, the lake is more yellow/brown than the channel, whereas if it is less than 1, the lake is more blue/green than the channel.

In **Figure 2a** and **2b**, which cover the same geographic extent on two different days, we show examples of two lakes, one with no channel connecting the lake and the river (A) and one with an obvious connection channel (B). The lake with clear channel presence frequently has a dominant wavelength of close to 1, indicating that the color of the lake and the color of the channel are similar though time (**Figure 2a & 2c**). The lake with no visible channel presence has a much wider distribution of dominant wavelength ratio values (**Figure 2d)**. When the river is transporting little sediment, the low connectivity lake and the channel look quite similar, but when the river water is high in sediment, the low-sediment lake looks very different from the channel (**Figure 2b**). As a result, we find that it is more effective to study distributions of dominant wavelength ratio within a time period as opposed to single instances in time in order to identify patterns of functional connectivity. The different time periods used in this study are described in Sections 3.3., 3.4., and 3.5.

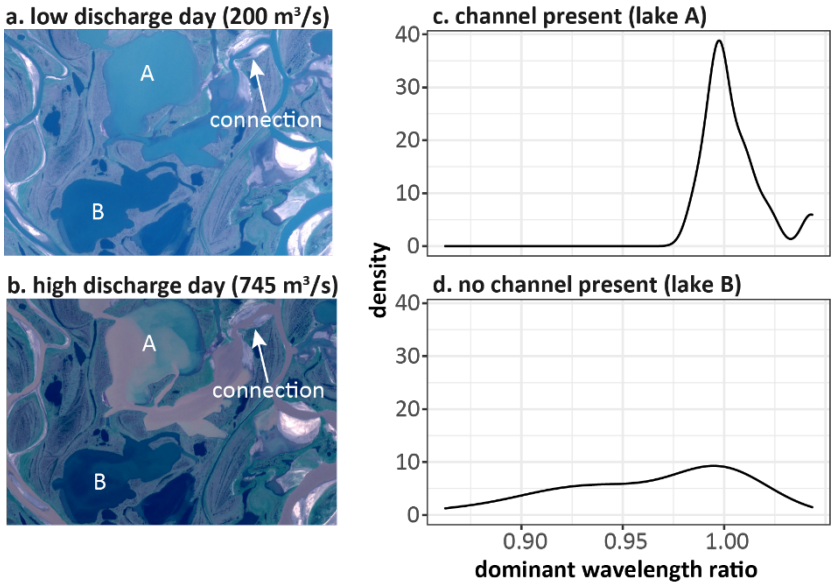

Figure 2. Sentinel-2 images from 7/14/2017-low discharge (a.) and 7/27/2017-high discharge (b.) showing lake color variability at different discharge levels. Example density plots using data from 2013-2016 for a lake A-visible channel (c.) and lake B-no visible channel (d.). Note the narrower shape of the density plot for the lake that has a channel present. Discharge values from USGS Gage 15875000 at Umiat, AK.

3.2.4. K-means clustering

Based on these distributions of dominant wavelength ratios, we group lakes into high functional connectivity and low functional connectivity groups. This method uses an unsupervised k-means approach developed specifically for clustering histograms (Irpino & Verde, 2015). We find that using three clusters best differentiates between lakes that do not routinely receive high sediment river water (classes 1 and 2) and those that do (class 3). Classes 1 and 2 are combined to form the 'low functional connectivity' class. An example of this clustering can be found in **Figure 3**. We tested our clustering algorithm using as many as ten clusters. Classifications using more than three clusters do not significantly increase classification accuracy and may result in overfitting. All dominant wavelength ratio distributions described in Sections 3.3., 3.4., and 3.5. are classified at the same time using the described algorithm.

Figure 3. Dominant wavelength ratio distributions and resulting classifications for lakes during the 2013–2016 time period. Classes 1 and 2 represent low functional connectivity lakes, whereas class 3 represents high functional connectivity lakes. Thick lines represent the centroid of each cluster.

3.3. Validation experiments (Q1)

To evaluate the accuracy of our classification algorithm, we compare the three validation datasets against functional lake connectivity based on classifications of dominant wavelength ratio distributions during corresponding time periods (**Table 1**). Distributions are only analyzed for a given lake if there are at least ten dominant wavelength ratio values within that period and the lake is contained in both our lake classification and the validation data set (see number of lakes validated in **Table 1**).

Table 1. Description of validation datasets, corresponding periods of functional connectivity analysis, and number of lakes validated.

Validation dataset	Validation data year	Functional connectivity time period	Number of lakes a
Jorgenson et al. (1997)	1992	2000-2004	82
Piliouras & Rowland (2020)	2014	2013-2016	97
GECI	2013-2016	2013-2016	83

3.4. Examination of temporal patterns in connectivity (Q2)

To better understand the variability of functional lake connectivity in the

Colville River Delta, we calculate dominant wavelength ratio values for each lake in four time periods: 2000-2004 (same distribution used in Section 3.3. for the Jorgenson et al., 1997 validation), 2005-2009, 2010-2014, and 2015-2019. We only analyze lakes that have at least 10 dominant wavelength ratio observations within all four periods (n=89 lakes). Each lake in each period is represented by a distribution of dominant wavelength ratios, all of which are included in the k-means clustering algorithm described in Section 3.2.4. This process results in a connectivity classification for each lake within each period. We use these classifications to better understand which lakes have static versus variable functional connectivity through time.

3.5. The impact of elevation and discharge on functional lake connectivity in the Colville Delta (Q3)

In this section we seek to better understand drivers of functional connectivity, starting with discharge. Using the USGS discharge data, we select the five years with the highest maximum summer discharge (2003, 2007, 2010, 2013, 2014) and the lowest maximum summer discharge (2006, 2008, 2015, 2017, 2019). We create two dominant wavelength ratio distributions for each lake, one for the low discharge years and one for the high discharge years. Only lakes with at least ten good dominant wavelength ratio observations in both the low and high discharge distributions are retained in the analysis (n= 95 lakes). These distributions are then included in the k-means clustering algorithm described in Section 3.2.4. This analysis helps better constrain how many and which lakes have connectivities that are influenced by discharge.

We also investigate patterns between connectivity and lake surface elevation using 2m-resolution ArcticDEM strip data described in Section 3.1.4. We compare lake surface elevations in 2015 and 2017 to connectivity in the 2015-2019 time period (n=88) and test for significance using a Mann-Whitney U-test.

3.6. Relationship between connectivity and lake ice (Q4)

To better understand the influence of connectivity on the deltaic environment, we compare functional connectivity to Landsat-derived lake ice climatology. The lake ice dataset was developed using a logistic regression based on a series of 2000–2019 Landsat 5/7/8 lake ice fraction observations, which was developed using a Landsat lake ice detection algorithm (Yang et al., 2021). For each lake, we pooled together all ice fraction data between 2000–2019 and divided the them into two subsets—one for freeze-up period (day of the year 230–365 and 1–58 of the following year) and one for the breakup period (day of the year 59–229). Then two separate logistic regressions were fitted to the two subsets of data to model the freeze-up and breakup ice fraction dynamics. These models together classify each day of the calendar year (DOY) as likely ice covered (typical ice fraction >80%), transitional (typical ice fraction 20-80%), or likely ice free (typical ice fraction <20%). We compare our functional connectivity results against ice phenology events including date of breakup transition start, date of breakup transition end, breakup transition duration, ice covered duration, ice

free duration, date of freeze-up start, date of freeze-up end, and freeze-up transition duration. Based on the temporal lake connectivity data from 3.4., lakes are divided into three groups for analysis: always high functional connectivity, always low functional connectivity, and variable functional connectivity. We use a Mann-Whitney U-test to compare ice climatology between high and low connectivity groups.

4. Results

4.1. Validation results (Q1)

Compared against channel absence/presence classifications from the GECI, functional connectivity classification matches with the channel presence classification in 85.5% of lakes (n=71/83). Of the incorrect classifications, only one lake with a visible channel is classified as low functional connectivity, whereas 11 lakes without channels are classified as high functional connectivity (**Figure 4a**). Amongst these lakes, over half (~7-8) are near the delta toe and may be brackish or experience non-channelized flooding due to their low elevations.

Next, we compared our 2013-2016 results to the 2014 classification of the Colville River Delta by Piliouras & Rowland (2020) (**Figure 4b**). This validation data set is similar to the Google Earth image-derived validation dataset because it defines connectivity via channel presence. In this case, channel presence was determined using 30m Landsat imagery. Our overall accuracy compared to this classification is 73.2%. Nearly all (n=24) of the 26 differently classified lakes are classified as high functional connectivity in our dataset but low functional connectivity by Piliouras & Rowland (2020). Most commonly, these are lakes with very narrow channels (less than one Landsat pixel wide) or dry channels at low discharge or are lakes near the delta toe that may easily experience overbank flooding.

Comparison of the 2000-2004 connectivity classification to the 1992 Colville Delta survey (Jorgenson et al., 1997, **Figure 4c**), yields an overall agreement of 69.5%, in which the classifications of 57 out of 82 lakes agree. Of the differently classified lakes, 4 lakes are classified as low functional connectivity in the validation dataset but high connectivity using our algorithm, and 21 are classified as high connectivity in the validation dataset but low functional connectivity using our algorithm. Nearly all of these 21 lakes are either within the 'deep tapped lake w/ high water connection' group (e.g. only receives river water at high discharge, n=13) or are connected to the channel network year-round but have channels that are either relatively narrow and long (n=6) or are indirectly connected to the main channel network via another lake (n=1). So, while these lakes may fall within the high connectivity validation group, they may not be functionally connected to the river network using our definition of connectivity. Additionally, the 1992 survey was 8 years prior to our first observation, and both lake tapping and lake or channel infilling are possible within this period.

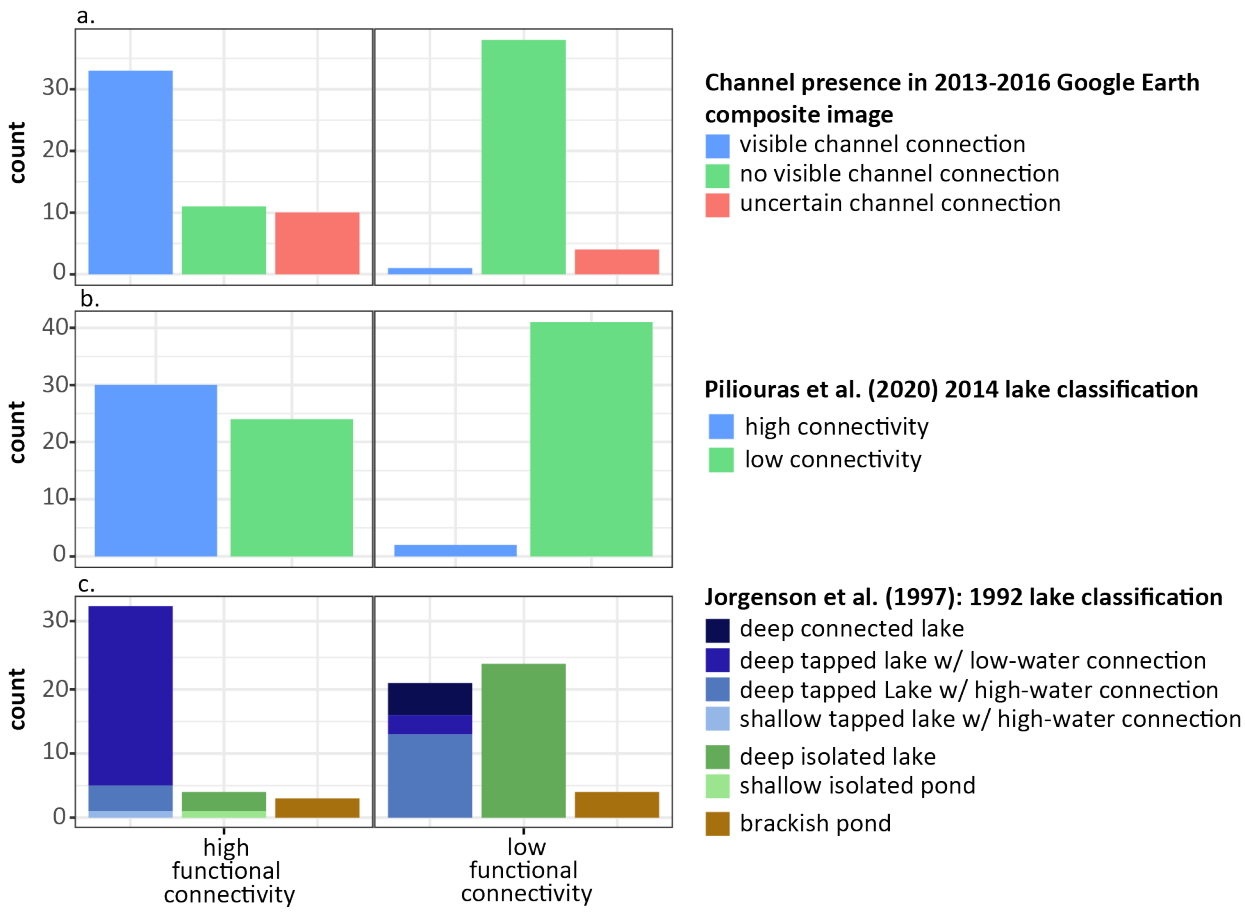

Figure 4. (a.) Comparison between manual channel identification in Google Earth Engine composite imagery and functional connectivity from the 2013-2016 period. (b.) Comparison between the 2014 (Piliouras & Rowland, 2020) classification and functional connectivity from the 2013-2016 validation period. (c.) Comparison between 1992 manual lake classification by Jorgenson et al. (1997) and functional connectivity from the 2000-2004 period.

4.2. Connectivity variability with time, discharge, and elevation (Q2-3)

Within the Colville Delta, functional connectivity remains consistent in the majority of lakes among the four five-year study periods between 2000 and 2019 (**Figure 5**). Of the observable lakes in the delta that had stable connectivity through time, more lakes were classified as always low functional connectivity (n=44) than always high connectivity (n=29). Of those that change connectivity through time (n=16), 2 transition from high to low connectivity over time, 5 go from low to high connectivity over time, and 9 lakes transition between one state and the other and back. These results help us to address Q2, regarding

temporal variability in functional connectivity.

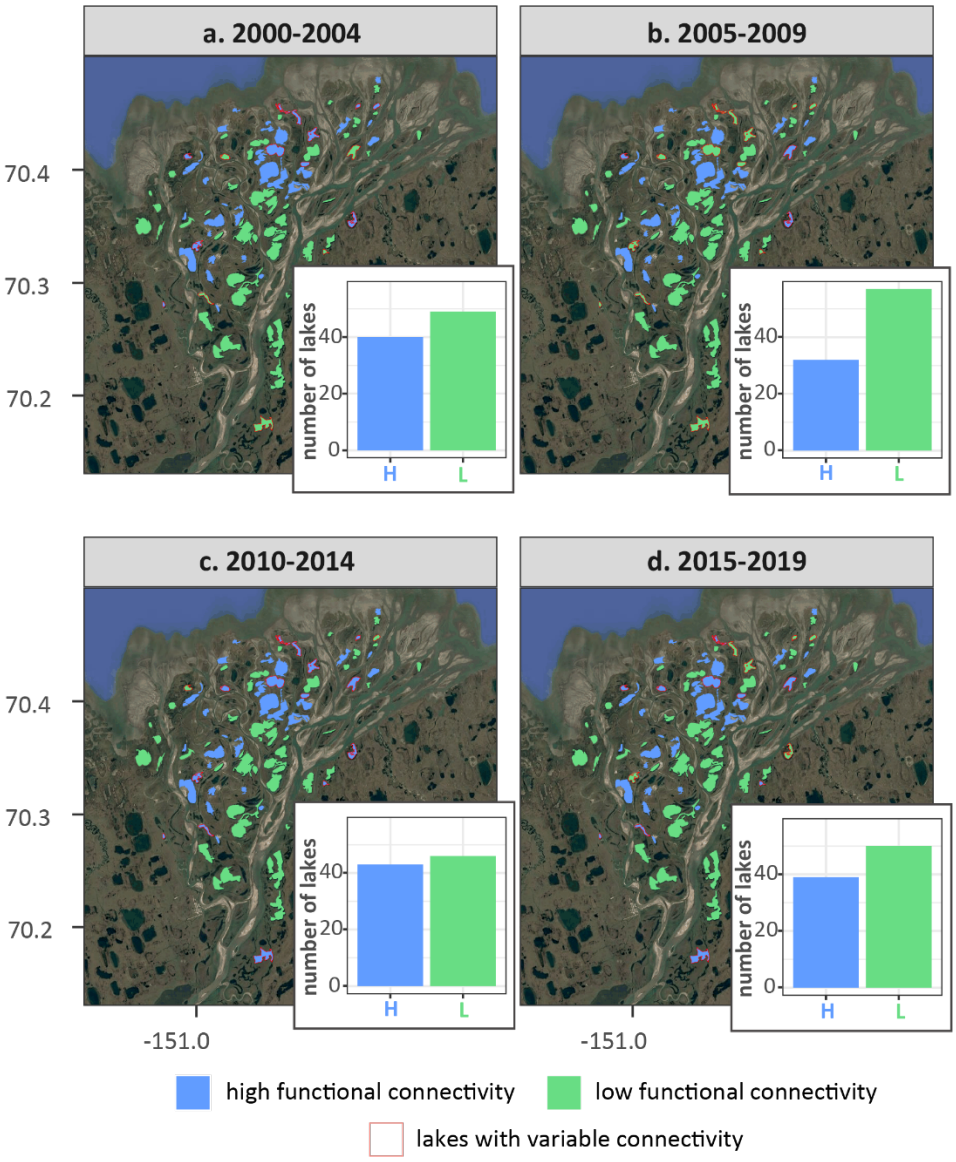

Figure 5. Landsat-derived connectivity classifications within four five-year study time periods. Lakes with variable connectivity across the four time periods are outlined in red on the maps.

When we compared lake functional connectivity during periods of high and low discharge, we identified 12 lakes that shift from high connectivity in high discharge periods to low connectivity in low discharge periods; there are no lakes with the opposing pattern (**Figure 6**). These two groups of lakes, those that

vary connectivity over time and those that vary connectivity through changes in discharge, often overlap (n=10 lakes are in both groupings), indicating that temporal changes in connectivity may be driven by discharge. The group of lakes experiencing the most variability in connectivity both over the whole study period and during the differing discharge periods are lakes that are either indirectly connected to the channel network via a long narrow channel or via other lakes, or are at very low elevation near the delta toe and may have more brackish influence or are more prone to non-channelized flooding. These results address the first part of Q3, on discharge impacts on connectivity.

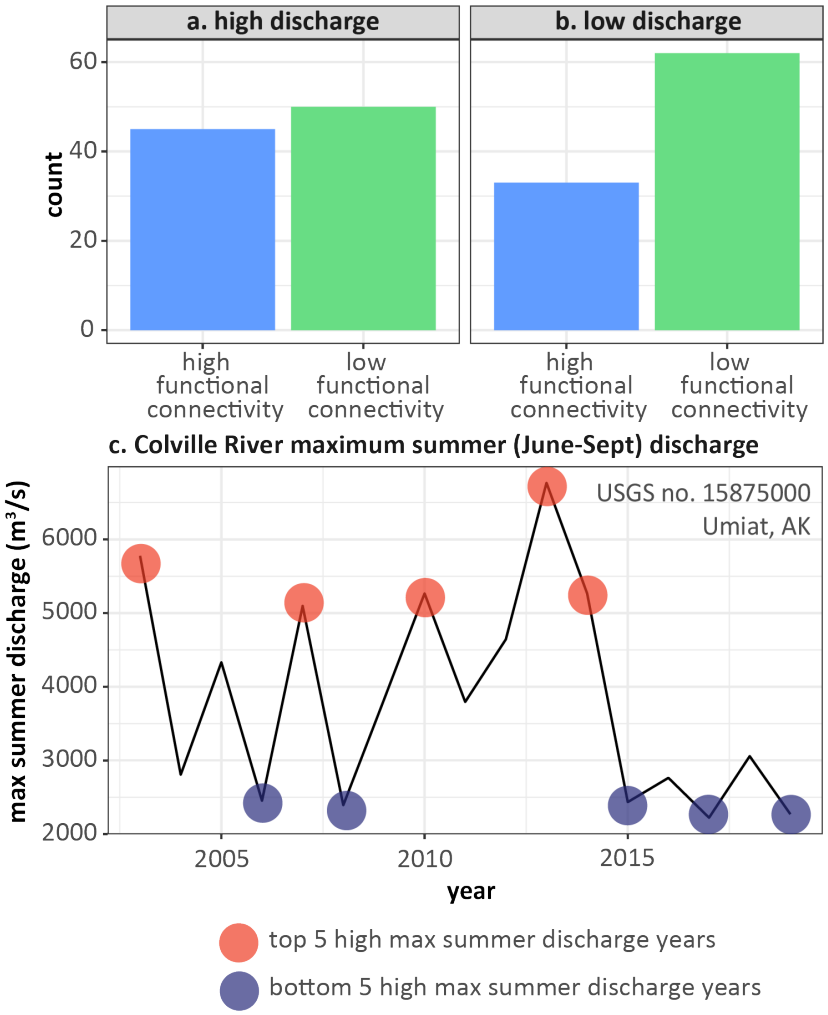

Figure 6. (a.) Lake connectivity classifications during the five years with the highest maximum summer (June-September) discharge. (b.) Lake connectivity classifications during the five years with lowest maximum summer discharge. (c.) Maximum summer discharge from 2003-2019 at USGS gage no. 15875000.

High (red) and low (blue) discharge years are indicated with colored circles.

As expected, high functional connectivity is also associated with significantly (p *<0.05*) lower wintertime lake surface elevation in both 2015 and 2017, compared to low functional connectivity lakes (**Figure 7,** 1.5m lower, on average, in both years). This makes sense from a definitional standpoint, as low elevation lakes are more likely to be flooded during periods of elevated river water level. Additionally, because the measured lake surface elevation reflects wintertime snow or ice cover elevation, the lower elevations of connected lakes may also reflect riverine drawdown of water from during the fall freeze-up process. These results address the second part of Q3, focused on elevation and connectivity.

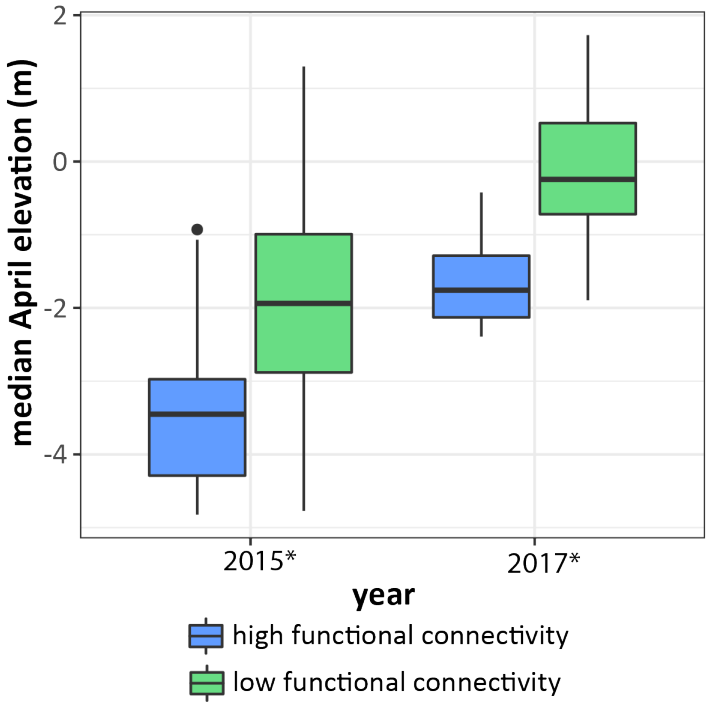

Figure 7. Lake surface elevation in the month of April from ArcticDEM. * indicates significant difference at p<0.05 between high and low functional connectivity lakes, as classified during the 2015-2019 period.

4.3. The relationship between connectivity and lake ice (Q4)

Within the Colville Delta, functional connectivity strongly correlates to lake ice climatology (**Figure 8**). In terms of breakup, results show statistically significant ($p < 0.05$) differences between always connected and always disconnected lakes in breakup transition start (always high functional connectivity lakes start breakup an average of 26 days earlier), breakup transition end (same, but 16 days earlier), and breakup transition duration (same, but 10 days longer). Regarding ice freeze-up, results show statistically significant differences in freeze-

up start day of year (always high functional connectivity lakes start freeze-up 8 days earlier), and freeze-up end (same, but 5 days earlier), but not freeze-up transition duration (same, but 4 days longer). Total ice duration (always high functional connectivity lake ice duration is 23 days shorter than always low functional connectivity lakes) and ice-free duration (same, but 21 days longer) are also significantly different. The ice phenology of lakes with variable functional connectivity nearly always falls between the average ice phenology for low and high connectivity lake groupings. Our analysis related to Q4 supports the hypothesis that ice duration and the ice breakup transition period are strongly influenced by connectivity.

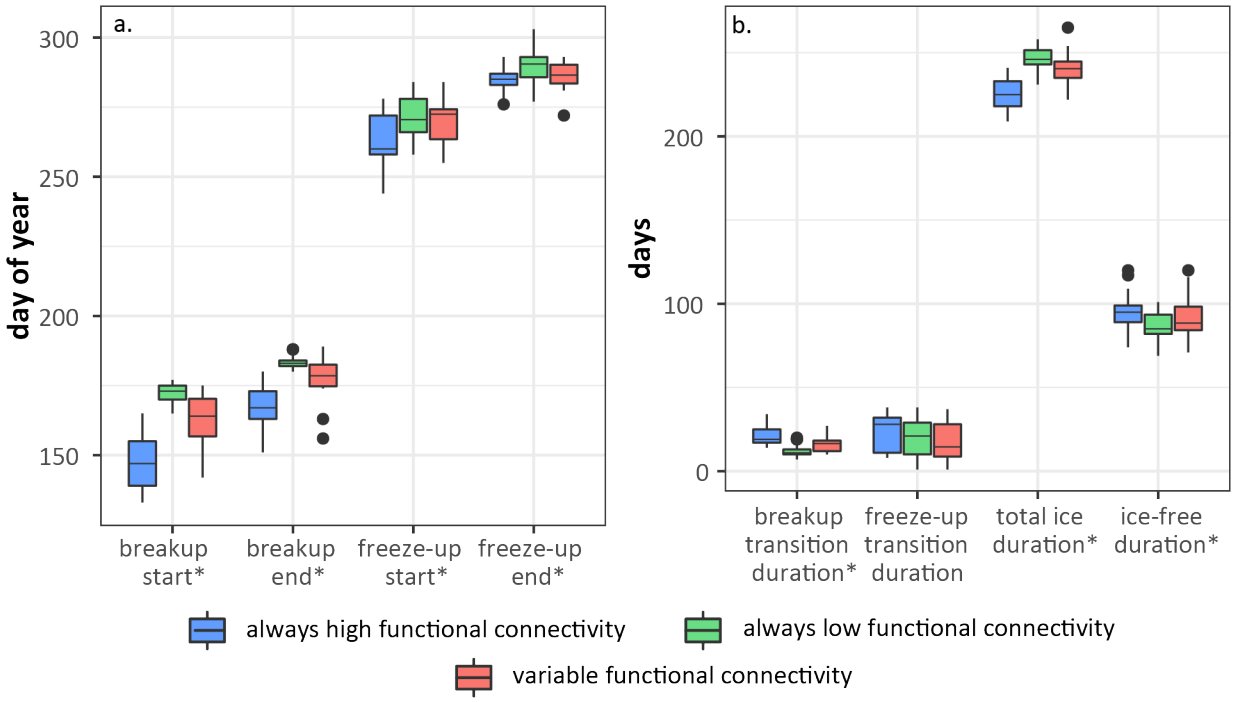

Figure 8. (a.) Lake ice breakup and freeze-up start and end dates for 89 lakes in the Colville River Delta. (b.) Lake ice durations (breakup transition, freeze-up transition, total ice, ice-free). *significant at p <0.05. Note the much earlier breakup start and end timing for high functional connectivity lakes.

5. Errors and Uncertainties

Functional connectivity detection via water color has certain limitations and potential sources of error. First, this method exclusively works when there is a visible difference in color between river water and lake water during at least some portion of the open water period. While this is true in the Colville Delta, deltas that export higher sediment overall, but have lower sediment concentrations, like the Lena Delta (Walker, 1998), would be difficult to analyze using

this method because of indistinct color difference between river water and lake water. In terms of potential sources of error, lakes can also experience non-SSC-driven changes in color, for example via high chlorophyll concentrations (Bukata et al., 1983; Jerome et al., 1994). While the DSWE algorithm used in this analysis to identify water pixels also filters out vegetated land pixels as well as submerged vegetation, it may not filter out other high chlorophyll water pixels. However, based on visible inspection of imagery, this seems to be a limited issue in the Colville Delta (no. of lakes possibly impacted ~2). Lakes near the delta toe present challenges in validation because they are likely both low elevation and brackish. These lakes commonly don't have clearly visible channels, so are not classified as connected in the Google Earth and Piliouras & Rowland (2020) validations, and are simply labeled as 'brackish', with no connectivity information, in the land survey validation dataset (Jorgenson et al., 1997). However, due to their low elevations, we expect that these lakes may still be functionally connected at high discharge because they can receive river water via overbank flooding. They are also close enough to the delta toe that seawater may impact the color of these lakes. Despite the potential for seawater influence, these delta toe lakes experience expected relationships with discharge, with high discharge periods leading to higher functional connectivity, and *vice versa*, leading to increased confidence in our classifications for these lakes.

Another potential source of error is in ice climatology calculations. While individual Landsat-derived ice fraction observations that go into creating the ice climatology model are dense during the breakup period, they are much less frequent during the freeze-up period due to low light and cloud conditions (**Figure 9**). Therefore, there is higher uncertainty/inaccuracy in climatological freeze-up dates compared to breakup dates. More specifically, for one week prior to the breakup start day of year through one week after the breakup end day of year, there are an average of 23 ice fraction observations used in the model, compared to an average of 8 for the freeze-up encompassing period. Also, because we are using a climatological timeseries constructed based on twenty years of data, distinguishing between a longer freeze-up/breakup period and a more variable freeze-up/breakup period is challenging.

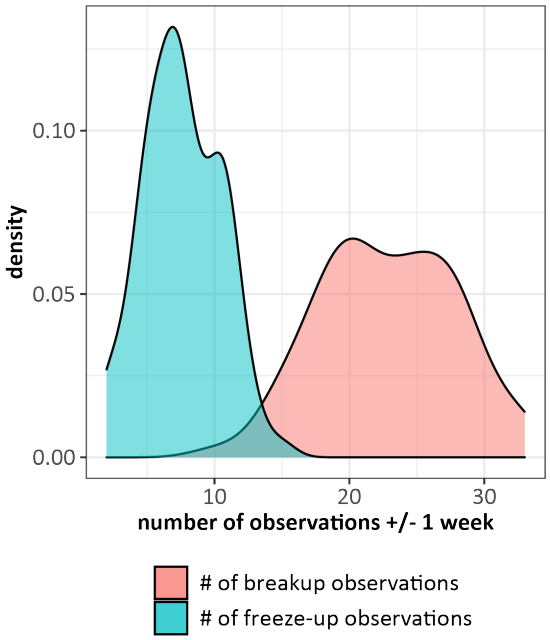

Figure 9. Number of Landsat ice observations used in the ice climatology model from one week prior to ice breakup/freeze-up start day of year to one week after breakup/freeze-up end day of year.

6. Discussion

The primary takeaways of this paper are threefold. First, we have demonstrated the efficacy of a widely applicable algorithm for detecting multi-temporal variations in functional connectivity in a high-sediment Arctic delta. Second, we find that over a twenty-year period connectivity in the Colville is variable through time in 20% of the lakes and is related to discharge as well lake elevation. Third, we find that functional connectivity may control ice timing, especially ice breakup, which has implications for photochemistry and methane production.

6.1. Efficacy of the functional connectivity algorithm

This functional connectivity algorithm provides a new alternative to other published deltaic connectivity detection methods. Each method is useful in specific situations and has unique pros and cons. Firstly, the 'Sill Elevation Method' used by Marsh & Hey (1989) and Lesack & Marsh (2010) uses lake sill elevations in combination with historical discharge observations to assess functional connectivity (by channel or overland flow) duration through time. This method is excellent in situations in which lake sill elevation data, collected via aerial or field survey, is available, and in situations when lake sill elevations are not assumed to change over the study period. While the reliance on aerial imagery or field data limits the wider spatial and temporal applicability, this method allows for the most temporally fine-grained analysis of functional connectivity

duration and allows calculation of connectivity prior to Landsat observations, if discharge data is available. Second, Piliouras & Rowland (2020) developed a method that uses Landsat imagery to detect direct connections between lakes and channels. While this algorithm was applied only within one year, it would be simple to expand temporally and has been expanded to multiple deltas and does not rely on the presence of high sediment river water. The challenge with this method is that it only detects connectivity via channels that are detectable within Landsat imagery, which excludes lakes connected by sub-pixel channels or by overland flow. The dominant wavelength ratio method described in our analysis builds on work by Long & Pavelsky (2013) that suggested the usefulness of suspended sediment as a tracer for river water recharge within six floodplain lakes in the Peace-Athabasca-Delta. In our dominant wavelength ratio method, similar to the Sill Elevation Method, we are able to detect functional connectivity either via channels or overland flow. Contrastingly, this method does not require aerial or field surveys to define sill elevation, and therefore is easier to expand to multiple deltas. However, unlike the Sill Elevation Method, this method doesn't allow detection of specific connectivity durations (e.g. 'whether a lake is connected for 4 or 40 days per year'). Compared to the Piliouras & Rowland (2020) method, our method allows for sub-pixel channel or overland flow-derived connectivity. However, the method described in this paper relies on river water with high sediment concentrations, limiting application to high sediment deltas. Additionally, our method results in connectivity classifications within coarser five-year periods. However, going forward, high temporal and spatial resolution optical satellites such as Sentinel-2 and Planet may be used to increase the temporal resolution of these connectivity classifications.

6.2. Discharge and connectivity

Our results highlight discharge as a major control on changes in functional connectivity, with high discharge corresponding to increased functional connectivity in the delta, and low discharge corresponding to reduced connectivity. These shifts are concentrated within two groups of lakes: those at low elevation near the delta toe and those that are connected to the main channel network indirectly via large lake complexes, long and narrow channels, or channels that are only water-filled at high discharge. While the North Slope region has not experienced a statistically significant trend in discharge over the past 41 years (1975-2015) (Durocher et al., 2019), future changes in precipitation type, timing, and amount, along with warmer air temperatures, are predicted to increase discharge on the North Slope over the next hundred years (Bring et al., 2017). Based on the pattern we have observed, projected increases in discharge could result in increased functional connectivity either via increased overland flow, higher sediment river water being transported further into lake complexes via channels, or lake tapping (Walker & McGraw, 2015). This increase in connectivity, particularly near the delta toe, will take place in conjunction with sea level rise, which will likely increase intrusion of saltwater into these low-elevation lakes, impacting the ecology and color of those systems (Jorgenson et al., 1997). Alternatively, increased SSC associated with elevated discharge

will also result in faster infilling of highly connected lakes (Walker & McGraw, 2015), leading to decreased connectivity. Any future changes in discharge will also be concurrent with degradation of permafrost (Hinzman et al., 2005). Permafrost degradation impacts Arctic lakes in several ways, including increased erosion rates (Piliouras et al., 2021), increased subsurface connectivity due to active layer thickening (Connon et al., 2014; Walvoord & Kurylyk, 2016), and resulting lake area loss and drainage (Smith et al., 2005; Marsh et al., 2009; Brubaker et al., 2014; Nitze et al., 2017) or expansion (Smith et al., 2005; Nitze et al., 2017). Residents of Nuiqsut are already reporting drying tributaries and loss of connectivity due to increased infilling and drainage as well as resulting concerns about fish migration and travel hazards (Brubaker et al., 2014).

6.3. Connectivity and lake ice

Air temperature is one of the dominant controls of lake ice phenology in conjunction with, to a lesser extent, lake morphometry, latitude, and elevation (Williams et al., 2004; Arp et al., 2013; Šmejkalová et al., 2016; Sharma et al., 2019; Warne et al., 2020). However, this work demonstrates the importance of functional connectivity as a driving factor of lake ice timing. This result fits well with initial findings by Arp et al. (2013) that suggests hydrologic connectivity may be responsible for intraregional lake ice variability in Alaska not explained by temperature or morphometric controls. Additionally, this corroborates results from Howell et al. (2009) that indicate river water acts as a mechanical and thermal instigator of ice breakup in Great Slave Lake, Canada. As lake ice continues to be modeled and interpreted both as a proxy for historical climate change (Robertson et al., 1992; Assel & Robertson, 1995; Magnuson et al., 2000; Prowse et al., 2011a; Šmejkalová et al., 2016 ; Warne et al., 2020) and as a signal of and response to current and future climate change (Arp et al., 2018; Sharma et al., 2019; Prowse et al., 2011a), and as we seek to quantify the impact of climate change on Arctic transportation (Prowse et al., 2009; Stephenson et al., 2011; Prowse et al., 2011b), it is important to consider functional connectivity as an input to lake ice models.

6.4. Potential impacts of connectivity on photochemistry and methane

Changes in connectivity, both through time and during differing discharge periods, are important from a carbon-cycle perspective. High functional connectivity lakes, by definition, receive increased levels of suspended sediment (Lesack & Marsh, 2010; Long & Pavelsky, 2013) and also have shorter water residence times (Coops et al., 1999, 2008; Lesack & Marsh, 2010). Suspended sediment is an extremely effective blocker of light (Vachon et al., 2017; Vione & Scozzaro, 2019). Increased levels of SSC result in less photosynthesis (Tank et al., 2009), lower macrophyte productivity (Lesack et al., 1998; Lesack & Marsh, 2010), less photomineralization. All of these differences result in less sequestration of CO_2 in high-SSC environments. Contrastingly, shorter residence times in these highly connected lakes means that any riverine DOC that arrives in these lakes will likely have relatively high photolability, similar to that of the river channel (Cory et al., 2014), leading to increased likelihood of full photomineralization

if there is enough UV radiation to penetrate more turbid waters. Poorly connected lakes lack riverine DOM input, but have been found to have increased macrophyte-derived DOM (Tank et al., 2009). As such, there are clear links between connectivity and the aquatic chemistry of Arctic lakes. The method developed in this paper to detect connectivity thus has potential application to understanding spatial and temporal variability in these processes.

7. Conclusions and future work

This research demonstrates the efficacy of using remotely sensed water color to detect spatial and temporal variations in functional lake connectivity in the Colville River Delta, Alaska. Results suggest that connectivity is variable in about 20% of delta lakes. Discharge is an important control of connectivity, particularly within those lakes that have indirect channel connections or are low elevation. Additionally, our results suggest a strong relationship between functional connectivity and lake ice phenology, especially observed earlier breakup timing in connected lakes. More fieldwork is needed to quantify the impact of this relationship on photochemistry and carbon processing in these lakes. In the future, we can use methods described in this paper to track connectivity in the Colville and other Arctic deltas and to understand how patterns of connectivity interact with the changing physical and biogeochemical environment of the Arctic.

Acknowledgments, Samples, and Data

We thank Dr. Anastasia Piliouras for providing MATLAB files containing connectivity information from Piliouras & Rowland (2020). Additionally, we acknowledge Dr. John Gardner for providing the DSWE algorithm implemented in Google Earth Engine and a version of the water color algorithm implemented in R. Finally, we acknowledge our primary funding source, NASA FINESST grant #80NSSC19K1344 (FI: Wayana Dolan, PI: Tamlin Pavelsky), and the UNC Preston Jones and Mary Elizabeth Frances Dean Martin Fellowship Fund.

R and Google Earth Engine scripts and input/output file descriptions can be publicly obtained on GitHub (https://github.com/whyana/colvilleConnectivity). All data used to run analyses are publically available on Zenodo (http://doi.org/10.5281/zenodo.5115099).

References

Allen, G. & Pavelsky, T. (2018). Global extent of rivers and streams. *Science,* 361, 585-588. https://doi.org/10.1126/science.aat0636

Amoros, C., & Bornette, G. (2002). Connectivity and biocomplexity in waterbodies of riverine floodplains. *Freshwater Biology,* 47, 761-776. https://doi.org/10.1046/j.1365-2427.2002.00905.x

Applied Climate Information System. ACIS Daily Data Browser, http://climate.gi.alaska.edu/acis_data, The Alaska Climate Research Center. Accessed March 25th, 2021.

Arp, C. D., Jones, B. M., & Grosse, G. (2013). Recent lake ice-out phenology within and among lake districts of Alaska, U.S.A. *Limnology and Oceanography,* 58(6), 2013-2028. https://doi.org/10.4319/lo.2013.58.6.2013

Arp, C. D., Jones, B. M., Engram, M., Alexeev, V. A., Cai, L., Parsekian, A., et al. (2018). Contrasting lake ice responses to winter climate indicate future variability and trends on the Alaskan Arctic Coastal Plain. *Environmental Research Letters,* 13, 125001. https://doi.org/10.1088/1748-9326/aae994

Assel, R. A., & Robertson, D. M. (1995). Changes in winter air temperatures near Lake Michigan, 1851-1993, as determined from regional lake-ice records. *Limnology and Oceanography,* 40(1), 165-176. https://doi.org/10.4319/lo.1995.40.1.0165

Boereboom, T., Depoorter, M., Coppens, S., & Tison, J.-L. (2012). Gas properties of winter lake ice in Northern Sweden: implication for carbon gas release. *Biogeosciences,* 9, 827-838. https://doi.org/10.5194/bg-9-827-2012

Bring, A., Shiklomanov, A., & Lammers, R. B. (2017). Pan-Arctic river discharge: Prioritizing monitoring of future climate change hot spots. *Earth's Future,* 5, 72-92. https://doi.org/10.1002/2016ef000434

Brubaker, M., Bell, J., Dingman, H., Itta, M., & Kasak, K. (2014). *Climate Change in Nuiqsut, Alaska.* ANTHC. http://anthc.org/wp-content/uploads/2016/01/CCH_AR_072014_Climate-Change-in-Nuiqsut.pdf

Bukata, R. P., Bruton, J. E., & Jerome, J. H. (1983). Use of Chromaticity in Remote Measurements of Water Quality. *Remote Sensing of Environment,* 13, 161-177.

Connon, R. F., Quinton, W. L., Craig, J. R., & Hayashi, M. (2014). Changing hydrologic connectivity due to permafrost thaw in the lower Liard River valley, NWT, Canada. *Hydrological Processes*, 28, 4163-4178. https://doi.org/10.1002/hyp.10206

Coops, H., Hanganu, J., Tudor, M., & Oosterberg, W. (1999). Classification of Danube Delta lakes based on aquatic vegetation and turbidity. *Hydrobiologia*, 415, 187-191. https://doi.org/10.1007/978-94-017-0922-4_26

Coops, H., Buijse, L. L., Buijse, A. D., Constantinescu, A., Covaliov, S., Hanganu, J., et al. (2008). Trophic gradients in a large-river Delta: ecological structure determined by connectivity gradients in the Danube Delta (Romania). *River Research and Applications*, 24, 698-709. https://doi.org/10.1002/rra.1136

Cory, R. M., Ward, C. P., Crump, B. C., & Kling, G. W. (2014). Carbon cycle. Sunlight controls water column processing of carbon in arctic fresh waters. *Science*, 345(6199), 925–928. https://doi.org/10.1126/science.1253119

Covino, T. (2017). Hydrologic connectivity as a framework for understanding biogeochemical flux through watersheds and along fluvial networks. *Geomorphology,* 277, 133-144. https://doi.org/10.1016/j.geomorph.2016.09.030

Dai, A., Qian, T., Trenberth, K. E., & Milliman, J. D. (2009). Changes in Continental Freshwater Discharge from 1948 to 2004. *Journal of Climate,* 22(10), 2773-2792. https://doi.org/10.1175/2008jcli2592.1

Denfeld, B. A., Baulch, H. M., del Giorgio, P. A., Hampton, S. E., & Karlsson, J. (2018). A synthesis of carbon dioxide and methane dynamics during the ice-covered period of northern lakes. *Limnology and Oceanography Letters,* 3(3), 117-131. https://doi.org/10.1002/lol2.10079

Department of Commerce, Community, and Economic Development. DCCCED Certified Population Counts (All Locations), https://dcra-cdo-dcced.opendata.arcgis.com/datasets/DCCED::dcced-certified-population-counts-all-locations/explore?location=70.224639%2C-150.758278%2C9.65, DRCA Data Portal. Accessed June 17th, 2021.

Durocher, M., Requena, A. I., Burn, D. H., & Pellerin, J. (2019). Analysis of trends in annual streamflow to the Arctic Ocean. *Hydrological Processes,* 33, 1143-1151. https://doi.org/10.1002/hyp.13392

Emmerton, C. A., Lesack, L. F. W., & Vincent, W. F. (2008). Mackenzie River nutrient delivery to the Arctic Ocean and effects of the Mackenzie Delta during open water conditions. *Global Biogeochemical Cycles*, 22, GB1024. https://doi.org/10.1029/2006gb002856

Ensom, T.P., Burn, C.R., & Kokelj, S.V. (2012). Lake-and channel-bottom temperatures in the Mackenzie Delta, Northwest Territories. *Canadian Journal of Earth Sciences*, 49, 963-978. https://doi.org/10.1139/E2012-001

Gardner, J. R., Yang, X., Topp, S. N., Ross, M. R. V., Altenau, E. H., & Pavelsky, T. M. (2021). The Color of Rivers. *Geophysical Research Letters*, 48, e2020GL088946. https://doi.org/10.1029/2020gl088946

Giardino, C., Kõks, K.-L., Bolpagni, R., Luciani, G., Candiani, G., Lehmann, M. K., et al. (2019). The Color of Water from Space: A Case Study for Italian Lakes from Sentinel-2. *Earth Observation and Geospatial Analyses of Earth Observation Data.* https://doi.org/10.5772/intechopen.86596

Hinzman, L. D., Bettez, N. D., Bolton, W. R. et al. (2005). Evidence and implications of recent climate change in Northern Alaska and other Arctic regions. *Climate Change,* 72, 251-298. https://doi.org/10.1007/s10584-005-5352-2

Howell, S. E. L., Brown, L. C., Kang, K.-K., & Duguay, C. R. (2009). Variability in ice phenology on Great Bear Lake and Great Slave Lake, Northwest Territories, Canada, from SeaWinds/QuikSCAT: 2000–2006. *Remote Sensing of Environment*, 113, 816-834. https://doi.org/10.1016/j.rse.2008.12.007

Irpino, A., & Verde, R. (2015). Linear regression for numeric symbolic variables: a least squares approach based on Wasserstein Distance. *Advances in Data Analysis and Classification*, 9, 81-106. https://doi.org/10.1007/s11634-015-0197-7

Jerome, J. H., Bukata, R. P., Whitfield, P. H., & Rousseau, N. (1994). Colours

of Natural Waters: 1. Factors Controlling the Dominant Wavelength. *Northwest Science,* 68(1), 43-52.

Jones, J. (2019). Improved Automated Detection of Subpixel-Scale Inundation—Revised Dynamic Surface Water Extent (DSWE) Partial Surface Water Tests. *Remote Sensing,* 11, 374. https://doi.org/10.3390/rs11040374

Jorgenson, T., Roth, J., Pullman, E., et al. (1997). *An ecological land survey for the Colville River Delta, Alaska, 1996.* Prepared for ARCO Alaska, Inc. and Kuukpik Unit Owners.

Karlsson, J., Giesler, R., Persson, J., & Lundin, E. (2013). High emission of carbon dioxide and methane during ice thaw in high latitude lakes. *Geophysical Research Letters,* 40, 1123-1127. https://doi.org/10.1002/grl.50152

Lauzon, R., Piliouras, A., & Roland, J.C. (2019). Ice and Permafrost Effects on Delta Morphology and Channel Dynamics. *Geophysical Research Letters,* 46, 6574-6582. https://doi.org/10.1029/2019GL082792

Lesack, L. F. W., & Marsh, P. (2010). River-to-lake connectivities, water renewal, and aquatic habitat diversity in the Mackenzie River Delta. *Water Resources Research,* 46, W12504. https://doi.org/10.1029/2010wr009607

Lesack, L. F. W., Marsh, P., & Hecky, R. E. (1998). Spatial and temporal dynamics of major solute chemistry among Mackenzie Delta lakes. *Limnology and Oceanography*, 43(7), 1530-1543. https://doi.org/10.4319/lo.1998.43.7.1530

Long, C. M., & Pavelsky, T. M. (2013). Remote sensing of suspended sediment concentration and hydrologic connectivity in a complex wetland environment. *Remote Sensing of Environment,* 129, 197-209. https://doi.org/10.1016/j.rse.2012.10.019

Magnuson, J. J., Robertson, D. M., Benson, B. J., Wynne, R. H., Livingstone, D. M., Arai, T., et al. (2000). Historical trends in lake and river ice cover in the northern hemisphere. *Science*, 289, 1743–1746.

Marsh, P., & Hey, M. (1989). The Flooding Hydrology of Mackenzie Delta Lakes near Inuvik, N.W.T., Canada. *ARCTIC,* 42(1), 41-49. https://doi.org/10.14430/arctic1638

Marsh, P., Russel, M., Pohl, S., Haywood, H., & Onclin, C. (2009). Changes in thaw lake drainage in the Western Canadian Arctic from 1950 to 2000. *Hydrological Processes,* 23, 145-158. https://doi.org/10.1002/hyp.7179

Mikhailova, M. V. (2009). Hydrological processes at an Arctic river mouth: Case study of the Colville River, Alaska, USA. *Water Resources,* 36(1), 26-42. https://doi.org/10.1134/s0097807809010035

Nitze, I., Grosse, G., Jones, B., Arp, C., Ulrich, M., Fedorov, A., & Veremeeva, A. (2017). Landsat-Based Trend Analysis of Lake Dynamics across Northern Permafrost Regions. *Remote Sensing,* 9, 640. https://doi.org/10.3390/rs9070640

Pekel, J.-F., Cottam, A., Gorelick, N., & Belward, A. S. (2016). High-resolution mapping of global surface water and its long-term changes. *Nature,* 540, 418-422. https://doi.org/10.1038/nature20584

Phelps, A. R., Peterson, K. M., & Jeffries, M. O. (1998). Methane efflux from high-latitude lakes during spring ice melt. *Journal of Geophysical Research: Atmospheres,* 103(D22), 29029-29036. https://doi.org/10.1029/98jd00044

Piliouras, A., & Rowland, J. C. (2020). Arctic River Delta Morphologic Variability and Implications for Riverine Fluxes to the Coast. *Journal of Geophysical Research: Earth Surface,* 125, e2019JF005250. https://doi.org/10.1029/2019jf005250

Piliouras, A., Lauzon, R., & Rowland, J. C. (2021). Unraveling the Combined Effects of Ice and Permafrost on Arctic Delta Morphodynamics. *Journal of Geophysical Research: Earth Surface,* 126, e2020JF005706 . https://doi.org/10.1029/2020jf005706

Porter, C., Morin, P., Howat, I. et al. (2018). ArcticDEM, Harvard Dataverse, V1. https://doi.org/10.7910/DVN/OHHUKH

Prowse, T., Alfredsen, K., Beltaos, S., Bonsal, B., Duguay, C., Korhola, A., et al. (2011a). Past and Future Changes in Arctic Lake and River Ice. *AMBIO,* 40, 53-62. https://doi.org/10.1007/s13280-011-0216-7

Prowse, T., Alfredsen, K., Beltaos, S., Bonsal, B. R., Bowden, W. B., Duguay, C. R., et al. (2011b). Effects of Changes in Arctic Lake and River Ice. *AMBIO,* 40, 63-74. https://doi.org/10.1007/s13280-011-0217-6

Prowse, T. D., Furgal, C., Chouinard, R., Melling, H., Milburn, D., & Smith, S. L. (2009). Implications of climate change for economic development in northern Canada: energy, resource, and transportation sectors. *Ambio*, *38*(5), 272–281.

Remmer, C. R., Owca, T., Neary, L., Wiklund, J. A., Kay, M., Wolfe, B. B., & Hall, R. I. (2020). Delineating extent and magnitude of river flooding to lakes across a northern delta using water isotope tracers. *Hydrological Processes,* 34, 303-320. https://doi.org/10.1002/hyp.13585

Robertson, D. M., Ragotzkie, R. A., & Magnuson, J. J. (1992). Lake ice records used to detect historical and future climatic changes. *Climatic Change,* 21, 407-427. https://doi.org/10.1007/bf00141379

Sharma, S., Blagrave, K., Magnuson, J. J., O'Reilly, C. M., Oliver, S., Batt, R. D., et al. (2019). Widespread loss of lake ice around the Northern Hemisphere in a warming world. *Nature Climate Change,* 9, 227-231. https://doi.org/10.1038/s41558-018-0393-5

Šmejkalová, T., Edwards, M. E., & Dash, J. (2016). Arctic lakes show strong decadal trend in earlier spring ice-out. *Scientific Reports*, 6, 38449.

Smith, L. C., Sheng, Y., MacDonald, G. M., & Hinzman, L. D. (2005). Disappearing Arctic Lakes. *Science*, 306, 1429. https://doi.org/10.1126/science.1108142

Stephenson, S. R., Smith, L. C., & Agnew, J. A. (2011). Divergent long-term trajectories of human access to the Arctic. *Nature Climate Change,* 1, 156-160. https://doi.org/10.1038/nclimate1120

Tank, S. E., Lesack, L. F. W., & Hesslein, R. H. (2009). Northern Delta Lakes as Summertime CO2 Absorbers Within the Arctic Landscape. *Ecosystems,* 12, 144-157. https://doi.org/10.1007/s10021-008-9213-5

U.S. Geological Survey. National Water Information System Data available on the World Wide Web (USGS Water Data for the Nation). Accessed June 18th, 2021.

Vachon, D., Solomon, C. T., & del Giorgio, P. A. (2017). Reconstructing the seasonal dynamics and relative contribution of the major processes sustaining CO2 emissions in northern lakes. *Limnology and Oceanography,* 62, 706-722. https://doi.org/10.1002/lno.10454

Vione, D., & Scozzaro, A. (2019). Photochemistry of Surface Fresh Waters in the Framework of Climate Change. *Environmental Science & Technology*, 53, 7945–7963. http://dx.doi.org/10.1021/acs.est.9b00968

Walker, H. J., United States. Office of Naval Research, & Louisiana State University and Agricultural and Mechanical College. Coastal Studies Institute. (1975). *The Colville River and the Beaufort Sea: Some Interactions.*

Walker, H. J. (1998). Arctic Deltas. *Journal of Coastal Research,* 14(3), 718-738. https://www.jstor.org/stable/4298831

Walker, H. J., & McGraw, M. (2015). Tapped lakes as sediment traps in an Arctic delta. *Proceedings of the International Association of Hydrological Sciences*, 367, 407-412. https://doi.org/10.5194/piahs-367-407-2015

Walker, H. J., Arnborg, L., & Peippo, J. (1987). Riverbank Erosion in the Colville Delta, Alaska. *Geografiska Annaler. Series A, Physical Geography.* https://doi.org/10.2307/521367

Walker, H.J., & Hadden, L. (1998). *Placing Colville Rover Delta Research on the Internet in a Digital Library Format.* Paper Presented at PERMAFROST Seventh International Conference, Yellowknife, Canada.

Walter Anthony, K. M., Vas, D. A., Brosius, L., Stuart Chapin, F., Zimov, S. A., & Zhuang, Q. (2010). Estimating methane emissions from northern lakes using ice-bubble surveys. *Limnology and Oceanography: Methods,* 8, 592-609. https://doi.org/10.4319/lom.2010.8.0592

Walvoord, M. A., & Kurylyk, B. L. (2016). Hydrologic Impacts of Thawing Permafrost-A Review. *Vadose Zone Journal,* 15(6). https://doi.org/10.2136/vzj2016.01.0010

Wang, J., Sheng, Y., Hinkel, K. M., & Lyons, E. (2011). Alaskan Lake Database Mapped from Landsat Images. Version 1.0. UCAR/NCAR – Earth Observing Laboratory. https://doi.org/10.5065/D6MC8X5R

Wang, S., Li, J., Shen, Q., Zhang, B., Zhang, F., & Lu, Z. (2015). MODIS-Based Radiometric Color Extraction and Classification of Inland Water With the Forel-Ule Scale: A Case Study of Lake Taihu. *IEEE Journal of Selected Topics in Applied Earth Observations and Remote Sensing,* 8(2), 907-918. https://doi.org/10.1109/jstars.2014.2360564

Warne, C. P. K., McCann, K. S., Rooney, N., Cazelles, K., & Guzzo, M. M. (2020). Geography and Morphology Affect the Ice Duration Dynamics of Northern Hemisphere Lakes Worldwide. *Geophysical Research Letters,* 47, e2020GL087953. https://doi.org/10.1029/2020gl087953

Wiklund, J. A., Hall, R. I., & Wolfe, B. B. (2012). Timescales of hydrolimnological change in floodplain lakes of the Peace-Athabasca Delta, northern Alberta, Canada. *Ecohydrology,* 5, 351-367. https://doi.org/10.1002/eco.226

Williams, G., Layman, K. L., & Stefan, H. G. (2004). Dependence of lake ice covers on climatic, geographic and bathymetric variables. *Cold Regions Science and Technology,* 40, 145-164. https://doi.org/10.1016/j.coldregions.2004.06.010

Yang, X., Pavelsky, T. M., Bendezu, L. P., & Zhang, S. (2021). Simple Method to Extract Lake Ice Condition From Landsat Images. *IEEE Transactions on Geoscience and Remote Sensing.* https://doi.org/10.1109/TGRS.2021.3088144